Journal of Electroanalytical Chemistry 712 (2014) 167–177

Contents lists available at ScienceDirect

Journal of Electroanalytical Chemistry

journal homepage: www.elsevier.com/locate/jelechem

Preparation and characterization of self assembled monolayers of 2-mercaptonicotinic acid on Au(1 1 1)

Diego E. Pissinis, Omar E. Linarez Pérez, Fernando P. Cometto, Manuel López Teijelo *

INFIQC – Departamento de Fisicoquímica, Facultad de Ciencias Químicas, Universidad Nacional de Córdoba, Haya de la Torre y Medina Allende, 5000 Córdoba, Argentina

ARTICLE INFO

Article history:
Received 29 April 2013
Received in revised form 5 November 2013
Accepted 12 November 2013
Available online 23 November 2013

Keywords:
Self-assembled monolayers
Aromatic thiols
Reductive desorption
SERS

ABSTRACT

The characterization by cyclic voltammetry, impedance spectroscopy and SERS measurements of 2-mercaptonicotinic acid (2-MNA) monolayers formed under different conditions on Au(1 1 1) surfaces, is reported.

Self-assembled 2-MNA monolayers on Au(1 1 1) in alkaline solutions desorbs reductively from the gold surface at −0.76 V (vs. ECS). From desorption experiments, the value of the surface concentration was estimated, resulting similar to that reported for related aromatic molecules.

Cyclic voltammetry (CV) and electrochemical impedance spectroscopy (EIS) show a rather imperfect blocking behavior of the 2-MNA SAMS. This behavior corresponds to that obtained for microelectrode arrays, which is attributed to the access of ions through pinholes, defects and/or pores present in the SAM.

The characteristics of ionisable groups exposed to the solution in the 2-MNA monolayers prepared by dipping in alkaline solutions were obtained by impedance measurements at different pH using the $[Fe(CN)_6]^{3-}/[Fe(CN)_6]^{4-}$ redox probe and the value of $pK_{a(SAM)}$ for the carboxylate group in the surface 2-MNA monolayer was estimated. For pH > pK_a, the carboxylic acid group is deprotonated and the monolayer acquires a negative surface charge, meanwhile it remains neutral or positively charged at lower pH values due to the beginning of pyridinic nitrogen protonation, which takes place overlapped with the protonation of the carboxylate group. The protonation of the pyridinic nitrogen is accompanied by desorption of this group from the surface. This leads to a change in the orientation of 2-MNA species allowing the interaction between the carboxylate group and the gold surface, which was further corroborated from SERS measurements.

In alkaline aqueous medium, 2-MNA adsorbs through a thiolate chemical bond on the gold surface and an additional interaction of the pyridinic nitrogen stabilizes the monolayer. One cathodic peak is obtained when reductive desorption is made in alkaline medium, while a splitting in two cathodic current contributions for pH values lower than ca. 7 indicates that two different molecular structures coexist on the gold surface in neutral or acidic media. This is assigned to the occurrence of an equilibrium between the molecular structure bonded through sulfur and nitrogen and the surface-bonded zwitterionic species by intramolecular proton transfer from the carboxylic acid group to the ring nitrogen, leading to the protonation of the pyridinic nitrogen and allowing the interaction of the carboxylate group with the gold surface.

1. Introduction

The self-assembling of organothiols on gold surfaces is one of the fascinating approaches for the development of chemically modified electrodes. These highly-organized monolayers can, in principle, provide the means to control the chemical and physical properties of the interfaces for a diversity of applications. Self-assembled monolayers (SAMs) of ω-functionalized alkanethiols have been widely used for the immobilization of proteins on electrode surfaces and they serve as ideal platforms for the construction of electrochemical biosensors.

Among the various studied SAMs, aromatic and heteroaromatic thiols/disulfides were of much interest in recent years [1–3], as the intermolecular interactions are expected to be different than those between alkanethiols, which may lead to different molecular packing of the structures. Higher electrical conductance would be expected in aromatic thiols, as the electrons are delocalized in the benzene ring [1]. The precise control of the surface properties (such as coverage and defects) of these functionalized monolayers is essential for the employment of SAM-modified surfaces for applications.

* Corresponding author. Tel.: +54 351 5353866; fax: +54 351 4334188.
E-mail address: mlopez@fcq.unc.edu.ar (M. López Teijelo).

1572-6657/$ - see front matter © 2013 Elsevier B.V. All rights reserved.
http://dx.doi.org/10.1016/j.jelechem.2013.11.013

The electron transfer blocking properties of alkanethiol/aromatic thiol monolayers are seldom perfect. In most cases, the behavior exhibited by monolayer-coated electrodes resembles an array of microelectrodes, where the active sites are identified as pinholes in the monolayer [4–17]. Both, the electrolyte and redox species in solution have access to the substrate at the pinholes. Pinholes are the result of imperfect adsorption of the alkanethiol to the surface during the self-assembly step and/or subsequent loss of the thiol during rinsing, storage, or use [18].

The acidity of surface-confined molecules is influenced by surface polarity, interfacial electrostatic field and local structure of the solvent [19]. It is generally observed that the measured pK_a of surface-confined molecules may differ significantly from the corresponding value for the same molecule in solution, which is ascribed to the influence of the local environment [19,20]. Acid/base ionization behavior of ω-functionalized SAMs of alkanethiols as well as of aromatic/heteroaromatic functionalized SAMs has been studied [21–40]. Nevertheless, the behavior of the –COOH and pyridinic groups as well as monolayer structure, orientation and electrochemical characteristics of SAMs of 2-mercaptonicotinic acid (2-MNA) on gold have not been reported.

Electrochemical techniques such as electrochemical impedance spectroscopy (EIS) and cyclic voltammetry (CV) are suitable techniques for monitoring the properties of self-assembled monolayers. They provide valuable information on the distribution of defects/holes, the properties of linked redox probes, the kinetics of the monolayer formation process and the surface coverage, among others [4–17,41]. Additionally, Surface-enhanced Raman scattering (SERS) has become an often used technique for obtaining information on the orientation of molecules adsorbed on metal surfaces [42–47].

In this paper, we report the characterization by cyclic voltammetry, impedance spectroscopy and SERS measurements of 2-MNA monolayers formed under different conditions on Au(1 1 1) surfaces.z

2. Experimental

2.1. Apparatus and electrodes

A conventional three-electrode electrolysis cell with a reference saturated calomel electrode (SCE) and a Pt auxiliary electrode was employed. All potentials are referred to the SCE potential. Working electrodes were deposits of Au on glass slides of 11 × 11 mm purchased from Arrandee or polycrystalline gold rods embedded in Teflon holders. The electrolyte was deaerated by bubbling with nitrogen prior to each experiment.

Cyclic voltammetry and Electrochemical Impedance Spectroscopy measurements were carried out with an Autolab PGSTAT100 electrochemical interface using the GPES (General Purpose Electrochemical System) and FRA (Frequency Response Analyzer) software packages. EIS measurements were recorded in the frequency range 0.01 Hz–100 kHz by applying a 10 mV-amplitude signal.

SERS experiments were performed ex situ (in air) using a Horiba LabRAM HR spectrometer, employing a He/Ne laser (632.8 nm wavelength). For the analysis of the spectra, the vibration modes are represented using the common nomenclature [42,48,49]: δ: bending; ν: stretching; τ: torsion; the subscript *as* indicates an asymmetric mode. Also, the nomenclature proposed by Wilson [48] and Lord [49] is indicated between parenthesis.

2.2. Preparation of the substrates

For the electrochemical measurements, the Au surface was electrochemically cleaned by 1 min cycling at 1 V s^{-1} between −1.2 V and 0.7 V in a 0.1 M NaOH solution. After that, the electrode was immersed in "piranha" solution (3:1 mixture of concentrated sulfuric acid and 30% hydrogen peroxide solution) during 1 min and rinsed with deionised water. In order to promote the development of the Au(1 1 1) surface, the electrode was annealed in a butane flame during two minutes, cooled under constant N_2 flux and placed immediately in contact with the dipping solution. In order to perform SERS measurements, a polycrystalline gold rod (Alfa Aesar, 99.9985% purity) was electrochemically cleaned by applying a potential step of +2.4 V during 10 min in a 0.5 M H_2SO_4 solution. Then, a linear potential sweep at 0.02 V s^{-1} from +2.4 V to −0.6 V was applied [44]. Finally, the highly roughened gold electrode generated after this procedure was rinsed with deionised water and immersed in the dipping solution.

2.3. Preparation of SAMs

All chemicals, 2-mercaptonicotinic acid (Alfa Aesar, 98 + % purity) and sodium hydroxide (Baker) were used as received without further purification. Self-assembled monolayers were prepared by immersing the previously annealed gold substrates in 10 mM 2-MNA + 0.1 M NaOH solutions during different dipping times (t_{dip}). After the surface modification, the samples were removed from the dipping solution, rinsed with deionised water and transferred to the electrolytic solution.

2.4. Reagents and solutions

In reductive desorption experiments, 0.1 M NaOH solutions deaerated by nitrogen bubbling were employed as electrolyte. Also, buffered 0.1 M NaH_2PO_4 (Baker) solutions (pH 2–13) were employed when necessary. For the electrochemical characterization using redox probes, 5 mM Fe^{+2}/Fe^{+3} (Baker) + 0.1 M H_2SO_4 (Anedra) solutions were employed. The titration curve was performed in a 5 mM $K_3Fe(CN)_6$ + 5 mM $K_4Fe(CN)_6$ (Baker) + 0.1 M Na_2SO_4 (Baker) solution. pH values in the 2–9 range were adjusted by adding H_2SO_4 or NaOH. For SERS measurements, the 2-MNA SAMs prepared on the roughened gold substrates were immersed during 15 min in 0.1 M NaOH or 0.1 M buffered phosphate (pH 4 or 7) solutions and rinsed with deionised water before the experiments.

3. Results and discussion

3.1. Voltamperometric characterization of 2-MNA SAMs

Electrochemical desorption of self-assembled monolayers from metal surfaces in aqueous alkaline solutions has been widely used to obtain information about the properties and structural characteristics of adlayers on metal substrates [50–54]. Fig. 1 shows the potentiodynamic *j*/*E* response obtained at 0.1 V s^{-1} by applying a triangular potential sweep in the −0.4 V to −1.3 V potential range in a 0.1 M NaOH solution, for a Au(1 1 1) substrate modified after 1 h of immersion in a 10 mM 2-MNA (pH 13) aqueous solution. Characteristic desorption/re-adsorption waves as well as the beginning of the hydrogen evolution reaction at ca. −1.2 V are seen (Fig. 1a). Negative scan shows a sharp main cathodic peak at −0.76 V (zone I) and a wide wave with several contributions in the −0.85 V to −1.2 V potential region (zone II). In the positive scan a poorly defined anodic contribution overlapped with the hydrogen evolution current is observed in the −0.85 V to −1.2 V range (zone III) while an anodic current peak at −0.6 V (zone IV) is also noticed.

In order to analyze the desorption response, baseline subtraction (Fig. 1b) and subsequent non-linear fitting using a Lorentzian

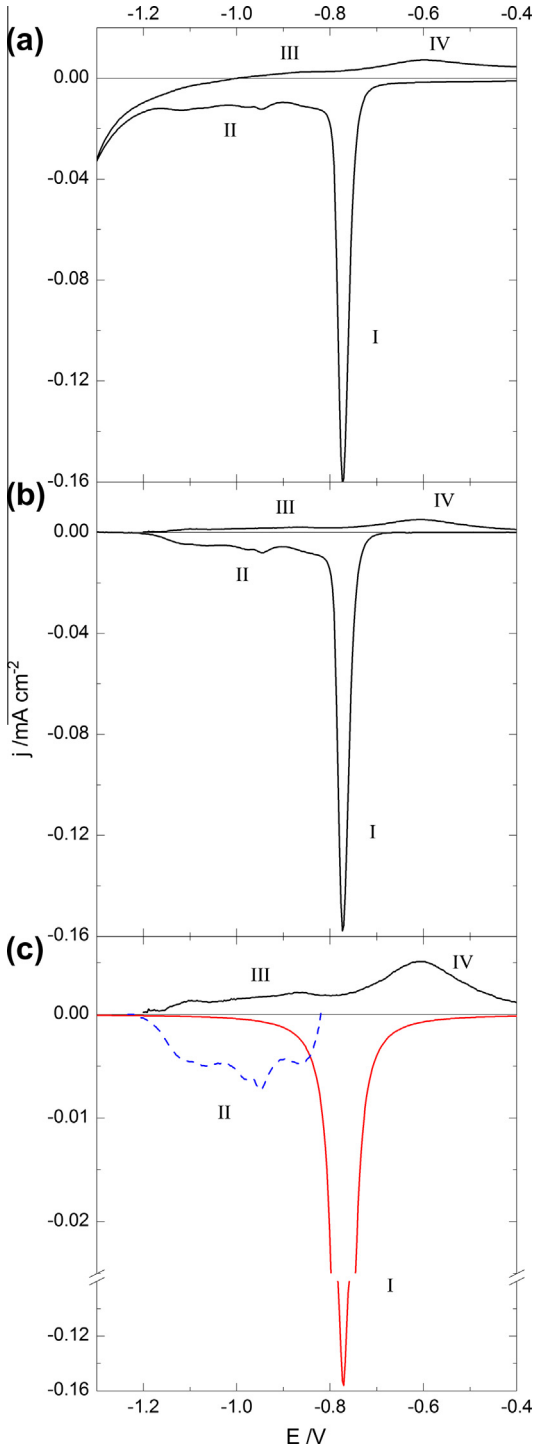

Fig. 1. Reductive desorption at 0.1 V s^{-1} in 0.1 M NaOH solution for a Au(1 1 1) electrode modified after 1 h of dipping in 10 mM 2-MNA (pH 13) solution. "As measured" response (a); after baseline subtraction (b) and after final signals deconvolution (c).

function were performed to the "as measured" response in the −0.7 V to −0.85 V potential range. Fig. 1c shows the final deconvolution at an enlarged current scale of the signals in zones I and II as well as the anodic contribution (zones III and IV) after applying this procedure.

The cathodic peak in zone I (peak I) is associated with the reductive desorption of the 2-MNA layer as thiolate species from the Au(1 1 1) surface, which can be readsorbed partially in the positive scan (zone IV). Only a small amount of thiolates are readsorbed, indicating that most of the species diffuse away from the surface due to the solubility of 2-MNA in aqueous media. This behavior is at variance with results for long-chain alkanethiols, which are insoluble in aqueous electrolytes. For the desorption peak I, peak potential (E_p), peak current (j_p), half-width peak ($\Delta E_{1/2}$) and desorption cathodic charge (Q_c) at different experimental conditions can be obtained. The average value of Q_c results 47.0 μC cm^{-2}, which is similar to values reported for other aromatic thiols at maximum coverage [31,32,51–54]. Assuming that one electron is involved in the desorption process for the Au-thiolate bond in alkaline aqueous solution as is usually made, a value for the surface concentration $\Gamma = 4.87 \times 10^{-10}$ mol cm^{-2} is obtained, which is similar to that reported for related molecules as 2-mercaptopyridine and 6-mercaptonicotinic acid [17,53].

It is well-known that the reductive desorption of a well ordered up-right monolayer of an alkanethiol with a $(\sqrt{3} \times \sqrt{3})R30°$ structure should produce a single sharp peak with values for desorption charge ranging from 75 to 85 μC cm^{-2} [32]. This value of charge corresponds to a coverage, based on the number of adsorbed molecules per number of substrate atoms in the unit cell, of 0.33 monolayers. Nevertheless, when the C atom bonded to the S head-group in aromatic thiolates presents a sp^2 hybridization, such as benzenethiolate on gold, Q varies from 45 to 56 μC cm^{-2} [31,55–57] and corresponds to a lower coverage than for aliphatic thiolates. In a recent paper, Matei et al. [58] found by means of XPS, LEED and STM experiments, that samples of 1,1′-biphenyl-4-thiol on Au(1 1 1) prepared from vapor phase (in vacuum) and liquid phase, form a hexagonal (2×2) structure at room temperature instead of the well-known $(\sqrt{3} \times \sqrt{3})$ structure. They relate the slightly increased molecular distances of the densely packed SAMs respect to the one for the typical $(\sqrt{3} \times \sqrt{3})$ structure of the densely packed alkanethiol SAMs on Au(1 1 1) to the increased van der Waals radii and intrinsic rigidity of the biphenyl-derived species [58]. Therefore, a value of 56 μC cm^{-2} instead 75 μC cm^{-2} is expected for the desorption charge in this kind of adsorbates, which would correspond to a coverage value of around 0.24. Nevertheless, it should be taken in mind that effects as penetration of water into the interfacial region due to the high solubility of the adsorbate as well as the repulsion produced by the presence of a negative charge on the carboxylate head group would also modify the size.

The origin of the cathodic contributions at potential zone II and its complementary contributions at zone III is not clear. It has been proposed for other aromatic thiols that the adsorption process induces activation of the oxidative cleavage of the S–C bond, with the resulting formation of an adlayer composed of atomic and oligomeric forms of sulfur [33,55,59–61].

In order to clarify the chemical origin of the current contributions in potential zone II, electrochemical and XPS studies of 2-MNA and Na_2S mixtures are in progress and the detailed study of this phenomenon will be discussed in a forthcoming paper.

As shown in Fig. 1, a cathodic peak at −0.76 V is obtained for the reductive desorption of 2-MNA layers in alkaline solutions for all the dipping times employed. Fig. 2a shows the deconvoluted j/E response at 0.1 V s^{-1} for SAMS obtained at different dipping times. Desorption charge (Q_c) increase and half-width peak ($\Delta E_{1/2}$) decrease with dipping time (Fig. 2b). For $t_{dip} \geqslant 30$ min, both Q_c and $\Delta E_{1/2}$ reach nearly constant values of 47.0 μC cm^{-2} and 27 mV respectively, indicating that 2-MNA molecules are closely packed on the Au surface and the structure of the SAM is nearly stabilized. Additionally, a linear dependence of the current density for the desorption peak, j_p, with the sweep rate, υ, as well as a constant desorption charge are obtained (results not shown) corroborating that only adsorbed species are involved in the cathodic process obtained at −0.76 V [62].

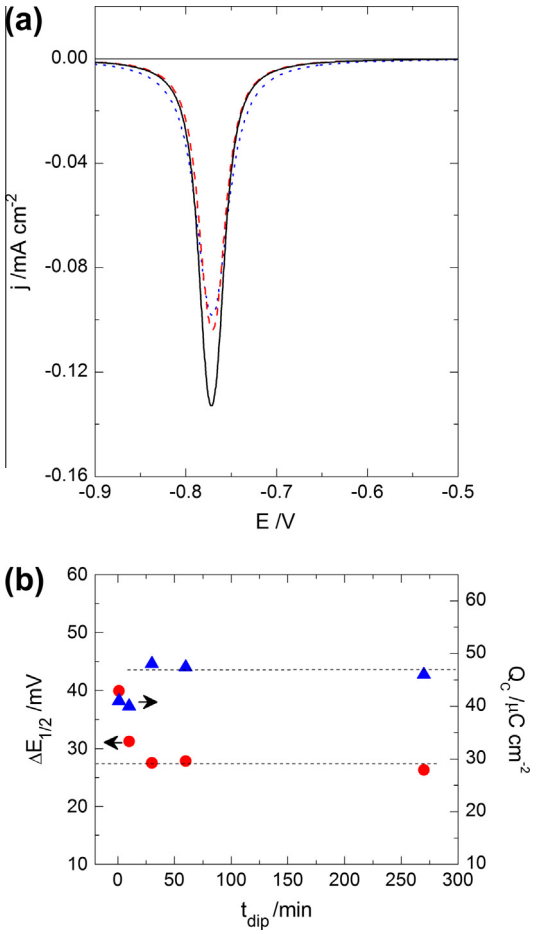

Fig. 2. (a) Deconvoluted reductive desorption profiles at 0.1 V s^{-1} in NaOH solution for a Au(1 1 1) electrode modified at different dipping times in 10 mM 2-MNA (pH 13) solution. t_{dip}: (••••••) 1 min; (– – – –) 10 min and (————) 60 min. (b) Dipping time dependence of the half width peak $\Delta E_{1/2}$ (●) and cathodic desorption charge Q_C (▲).

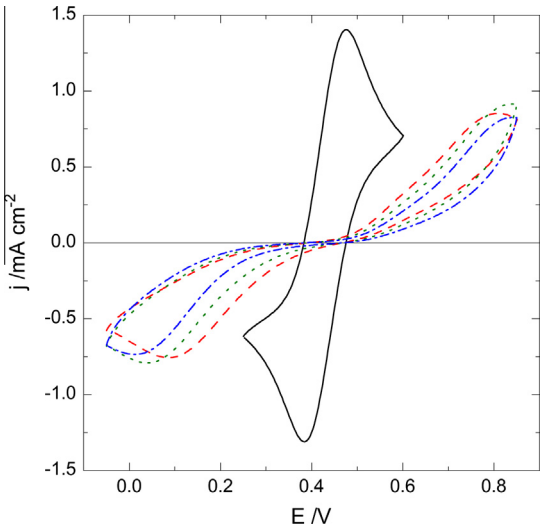

Fig. 3. Potentiodynamic j/E response at 0.1 V s^{-1} in 10 mM Fe^{2+}/Fe^{3+} + 0.1 M H_2SO_4 for bare (————) and modified Au(1 1 1) electrodes for different dipping times in 10 mM 2-MNA (pH 13). t_{dip}: 15 min (– – – –); 1 h (••••••) and 6 h (– • – • –).

3.2. Fe^{2+}/Fe^{3+} redox couple electrochemical behavior on 2-MNA SAMs

Usually, well-behaved redox couples are employed to sense the electrochemical activity of an electrode surface. In the presence of SAMs, the change of the kinetics of the electron transfer reaction provides structural information of the films [4–17].

Cyclic voltammetry is an important technique to evaluate the blocking properties of monolayer-coated electrodes using diffusion-controlled redox couples as probes. Fig. 3 shows the potentiodynamic j/E response at 0.1 V s^{-1} of bare and modified Au(1 1 1) electrodes in 10 mM Fe^{2+}/Fe^{3+} + 0.1 M H_2SO_4 solutions for different dipping times. On bare Au(1 1 1) surface, the Fe^{+2}/Fe^{+3} redox couple shows a quasi-reversible j/E response, with ca. 90 mV of anodic to cathodic peak potentials separation, ΔE_p, and the typical shape for a charge transfer process controlled by semi-infinite linear diffusion [63]. On the other hand, the potentiodynamic j/E response of modified Au(1 1 1) surfaces at different dipping times shows a pronounced increase of ΔE_p (ranging from 750 mV for 15 min to 830 mV for 6 h of dipping time) and a decrease of the peak current for both the anodic and the cathodic peaks. No apparent changes in the monolayer structure such as desorption or oxidation are noticed in the potential range employed. This rather imperfect blocking behavior corresponds to that obtained for microelectrode arrays [5]. This microelectrode array behavior is attributed to the access of ions through pinholes, defects and/or pores present in the SAM, which facilitates radial diffusion of the redox probe species as opposite to linear diffusion observed for the case of bare gold surfaces [4,5]. Nevertheless, properties of SAMs such as surface coverage or distribution of pinholes and defects are obtained much more easily from impedance analysis.

Electrochemical impedance spectroscopy is also a powerful technique to probe surface modified electrodes, providing information on solution resistance, double layer capacitance, diffusion processes and charge transfer process occurring at SAM modified surfaces. Fig. 4 shows the Nyquist diagrams of the impedance response obtained in 10 mM Fe^{2+}/Fe^{3+} + 0.1 M H_2SO_4 solutions for bare (inset) and modified Au(1 1 1) electrodes at different dipping times. At high frequencies the spectrum for the bare gold surface shows one RC semicircle followed by a straight line with 45° slope at low frequencies. This is the typical impedance behavior for a charge transfer reaction controlled by semi-infinite linear diffusion and it is usually interpreted in terms of the Randles equivalent

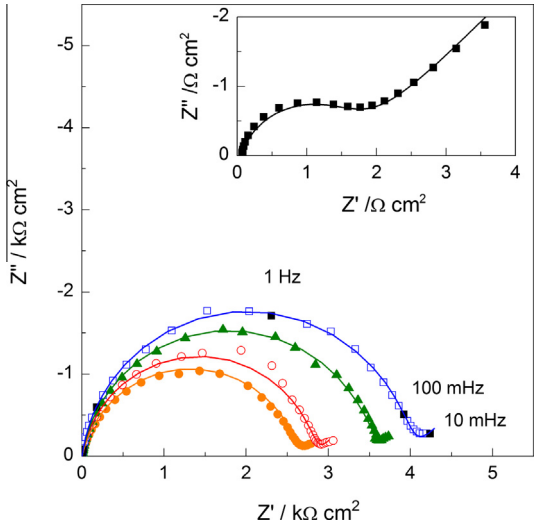

Fig. 4. Nyquist diagrams in 10 mM Fe^{2+}/Fe^{3+} + 0.1 M H_2SO_4 of bare (inset) and modified Au(1 1 1) electrodes for different dipping times in 10 mM 2-MNA (pH 13). t_{dip}: 5 min (●); 15 min (○); 1 h (▲) and 6 h (□). Full lines: simulations after fitting with the Randles circuit.

electrical circuit [64]. Values for the double layer capacitance of the electrode surface, C_{dl}, charge transfer resistance related to the kinetic constant for the electrochemical reaction, $R_{ct,bare}$, and Warburg diffusional parameter, σ, can be obtained from fitting procedures employing the Randles circuit. On the other hand, the impedance response for the modified Au(1 1 1) surfaces shows only the RC semicircle at high frequencies but the diffusion regime is not clearly defined at low frequencies. It can be seen that the diameter of the semicircles ($R_{ct,SAM}$) is always of higher size than that obtained for the bare Au surface and increases as dipping time increases. $R_{ct,SAM}$ values were also obtained from fitting employing the Randles circuit. Higher $R_{ct,SAM}$ values indicate a decrease in the electron transfer reaction rate or a diminution of the active area. The last assumption can be taken into account as a decrease in the apparent value for the electron transfer rate constant due to the non-perfect monolayer structure, since pinholes and other defects may exist as a result of imperfect adsorption of molecules during the self-assembly step and/or subsequent loss of molecules.

In order to characterize a modified surface it is important the determination of nature, size and distribution of the pinholes or other defects as well as coverage. One of the simplest models found in literature treats the pinholes as an array of microelectrodes of uniform size and spacing distributed in an insulating plane, where the coverage, θ, is defined by geometrical considerations [5]. Radial diffusion to the pinholes in the SAM dominates the overall behavior and, under these conditions, the current is not a simple function of the exposed area of the coated electrode. It has been shown [5] that for modified electrodes with $\theta > 0.9$, the charge transfer resistance, $R_{ct,SAM}$, is related to the covered surface fraction by the equation:

$$\theta = 1 - \frac{R_{ct,bare}}{R_{ct,SAM}} \quad (1)$$

from which an estimation of coverage was made. An increase of the coverage value from $\theta = 0.9994$ to 0.9996 for 5 min to 6 h dipping times, respectively, is obtained. This variation indicates that a higher stabilization and packing of the monolayer is obtained as dipping time increases. As a conclusion, 2-MNA molecules adsorb on Au(1 1 1) at high coverage forming a closely packed structure and presenting also the characteristics of an array of microelectrodes due to the existence of pinholes and/or other defects. However, the values of coverage should be taken judiciously since they can be overestimated due to the existence of monolayer charge effects (see below).

The analysis of size and distribution of pinholes and defects of the monolayer cannot be performed since the information necessary is contained in the low frequency region of the impedance spectra where the diffusion effects are important, which are not clearly defined in the present case.

3.3. Characterization of adsorption process of 2-MNA on Au(111)

In aqueous solution, 2-mercaptonicotinic acid behaves as a weak acid presenting a complex behavior. Multiple acid–base equilibrium reactions as shown in Scheme 1 have been reported [65]. Based on the neutral molecular form of 2-MNA, similar values of $pK_{a2} = 5.8$ and $pK_{a3} = 8.8$ and a substantially lower value $pK_{a1} = 0.88$ have been found by spectroscopic measurements [66]. Nevertheless, from potentiometric titration data pK_a values of 7.4 and 11.0 for the carboxylic and thiol groups have also been reported recently [67]. Apart from the acid–base equilibrium reactions shown in Scheme 1 and 2-MNA presents equilibrium reactions between different tautomeric species involving the formation of thione groups similar to those described for 2-mercaptopyridine and 2-mercaptopyrimidine [68]. Furthermore, pyridinecarboxilic acids can also exist as tautomeric mixtures of neutral and zwitterionic forms in aqueous or aqueous/organic solvent mixtures [66]. For 2-MNA, tautomeric equilibrium constant for zwitterion formation as well as the values of the acid–base dissociation constants were determined, concluding that 2-MNA exists predominantly as the zwitterion form in the mixtures investigated [66].

2-Mercaptonicotinic acid molecules present four chemical groups which may function as ligands in the surface adsorption process, i.e. the sulfur atom, the carboxylic group, the nitrogen in the pyridinic ring and the aromatic π system. The usual practice

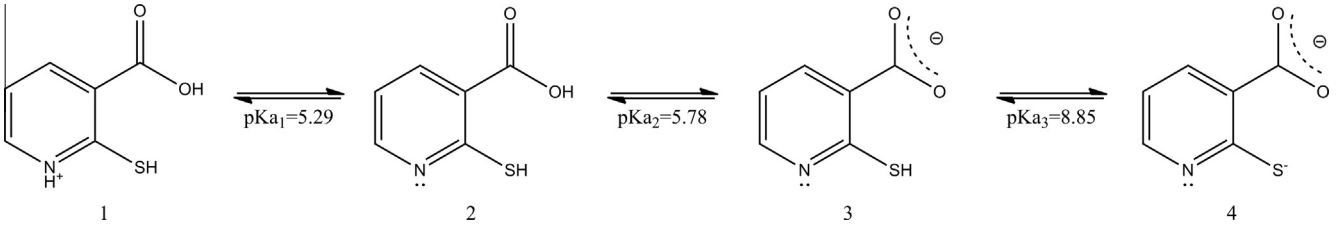

Scheme 1. 2-MNA acid–base equilibria in aqueous solutions.

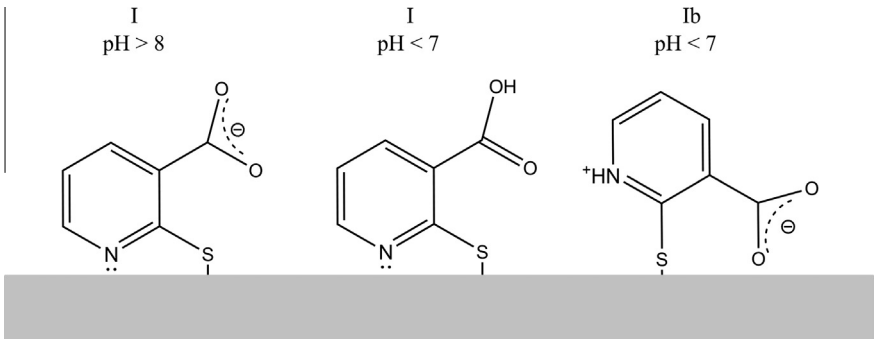

Scheme 2. Schematic representation of the possible configurations for 2-MNA adsorption onto Au(1 1 1) at different pH values.

is to prepare the monolayers in strong alkaline aqueous solutions. Under these conditions, 2-MNA stable species corresponds mainly to the doubly-charged negative species (structure 4 in Scheme 1), and/or the thione tautomeric species. As a strong thiolate-gold chemical bond is expected for the experimental dipping conditions employed, after adsorption the thione species can be discarded for the 2-MNA adsorbed surface species. In addition, a moderate interaction involving the non-bonding electrons of the non-protonated pyridinic nitrogen with the gold surface could stabilize the molecular adsorption. It has been reported that related molecules such as 2-mercaptopyridine or 6-mercaptonicotinic acid assemble on gold surfaces through sulfur and nitrogen atoms, adopting a near-vertical orientation [17,53].

Surface enhanced Raman scattering has been established as a powerful tool for the spectroscopic investigation of adsorbate–metal interactions. Therefore, in order to obtain independent information regarding 2-MNA adsorption on gold surfaces, SERS measurements have been performed. Fig. 5 shows Raman spectra obtained for an aqueous alkaline (pH 13) 2-MNA solution (Fig. 5a) compared with SERS spectra for 2-MNA monolayers prepared under different conditions. SERS spectrum of a monolayer obtained by dipping in a 2-MNA solution at pH 13 is shown in Fig. 5b, while typical results recorded for monolayers prepared at pH 13 and afterwards immersed in acidic (pH 4) or neutral (pH 7) solutions, which were very similar, are shown in Fig. 5c.

The comparison of the conventional Raman spectrum of 2-MNA in solution (Fig. 5a) with SERS spectra of 2-MNA monolayers under different conditions (Fig. 5b and c), shows a shifting of peak positions of 5–20 cm^{-1} and a relative enhancement of multiple signals. This shifting in peak positions indicates that 2-MNA molecules are chemisorbed on the modified gold surface. Most of the "in plane" ring vibration modes are present and result enhanced: δCH(18b) at 1049–1053 cm^{-1}; νCC (8a) at 1591–1600 cm^{-1}; νCC(19b) at 1443–1450 cm^{-1}; ν_{as}CH(13) at 1118–1123 cm^{-1}; νCC(1) at 1077–1080 cm^{-1}; δCC(6a) at 625–646 cm^{-1}. In addition, the absence of the "out of plane" modes τCCCC (16b) at 431–477 cm^{-1} and τCCCC (4) at 733 cm^{-1} is noticed. Additionally, for SAMS obtained by dipping in 2-MNA solutions at pH 13 (Fig. 5b) the lack of carboxylate stretching ($\nu_s COO^-$ at 1383 cm^{-1}) and bending (δCOO^- at 854 cm^{-1}) vibrations indicates that in alkaline solutions no interaction of the carboxylate group with the gold surface is detected by SERS. The strong enhancement of the "in-plane" ring vibrations as well as the absence of carboxylate stretching or bending signals in alkaline medium points to the 2-MNA molecules adsorption perpendicularly to the Au(1 1 1) surface through a thiolate-gold covalent bond as well as by a weak interaction of the non-protonated pyridine nitrogen, leaving the carboxylate group exposed to the solution (see Scheme 2).

3.3.1. Impedance titration

In order to determine the existence of ionisable groups exposed to the solution in the 2-MNA monolayers prepared by dipping in alkaline solutions (pH 13), impedance measurements using the $[Fe(CN)_6]^{3-}/[Fe(CN)_6]^{4-}$ redox probe were performed varying the pH of the electrolyte in the 2–10 range. Impedance spectra were measured at the formal potential corresponding to the $[Fe(CN)_6]^{3-}/[Fe(CN)_6]^{4-}$ redox couple and the values of R_{ct} were obtained from fitting employing the Randles circuit as described in Section 3.2. Thus, 2-MNA monolayers can be titrated by changing the solution pH since the charge density at the monolayer changes and, consequently, R_{ct} changes as well. The values of R_{ct} for the redox couple at the bare Au(1 1 1) surface at the different pH values were also obtained.

Fig. 6 shows the variation of R_{ct} with pH, measured on the bare and the modified Au(1 1 1) surfaces by 1 h dipping in 10 mM 2-MNA (pH 13) solution. As can be seen, values of R_{ct} obtained for the modified surface increase with pH due to the inhibition of the electron transfer rate following a broad sigmoid response, which is characteristic of a typical titration curve. This variation takes place as a result of the increase in electrostatic repulsion between the negatively charged species of the redox probe and the surface charge density on the monolayer as pH increases

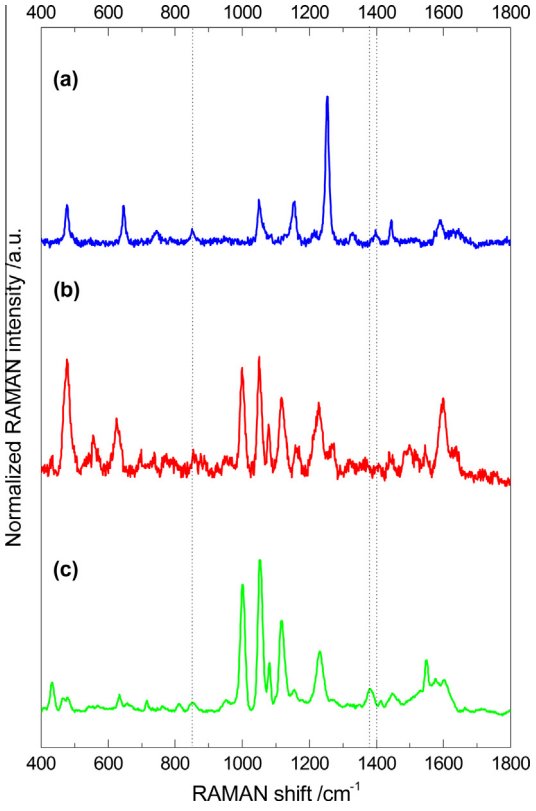

Fig. 5. Raman spectra for 0.1 M 2-MNA (pH 13) aqueous solution (a); 2-MNA SAMs on Au prepared by 1 h dipping in 0.1 M NaOH (pH 13) (b); and immersed subsequently for 10 min in solutions of pH 7 or 4 (c).

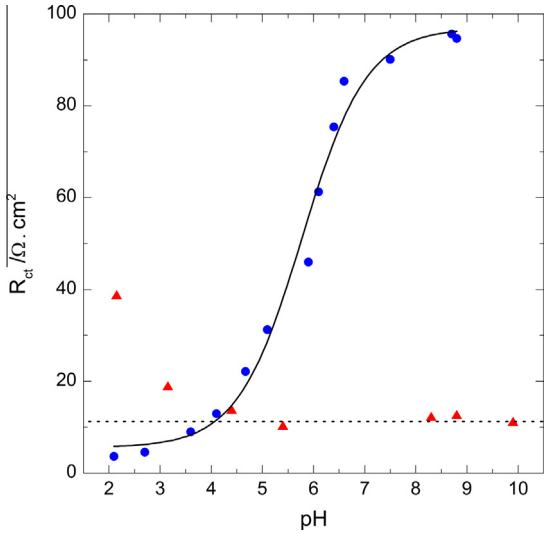

Fig. 6. Impedance titration curve measured using $[Fe(CN)_6]^{3-}/[Fe(CN)_6]^{4-}$ as a redox probe on bare (▲) and modified Au(1 1 1) surfaces (●) by 1 h dipping in 10 mM 2-MNA (pH 13) solution.

[17,69–71]. From the inflexion of the titration curve, a value $pK_{a(SAM)} \approx 6.0$ can be estimated for the surface 2-MNA monolayer.

This result indicates that for pH > pK_{a2}, the carboxylic acid group is deprotonated and the monolayer acquires a negative surface charge, meanwhile it remains neutral or positively charged at lower pH values (Fig. 6) due to the beginning of pyridinic nitrogen protonation. Additionally, the dependence with pH of the charge transfer resistance for the bare gold surface, $R_{ct,bare}$, deserves a careful analysis. For pH ⩾ 5, $R_{ct,bare}$ has a constant value of ≈ 11 Ω cm^2, while for pH ⩽ 4.5 increases reaching a value ≈ 40 Ω cm^2 for pH 2. This can be explained taking into account the pH effect on the kinetics of electron transfer of the redox probe. Holzwarth et al. [72] have studied the pH dependence of the kinetic parameters for the $[Fe(CN)_6]^{3-}/[Fe(CN)_6]^{4-}$ electron transfer reaction in aqueous solutions. They reported that below pH 5, $[Fe(CN)_6]^{4-}$ species can be protonated to $H[Fe(CN)_6]^{3-}$ and $H_2[Fe(CN)_6]^{2-}$, being the $[Fe(CN)_6]^{3-}$ species the only oxidation product. As a consequence, because a previous deprotonation process must take place, the electron transfer rate constant decreases as pH is lowered and, consequently, the increase of $R_{ct,bare}$ below pH 5 is seen (Fig. 6).

From the comparison of R_{ct} variation with pH obtained for the bare and modified gold surfaces, two different pH zones can be distinguished. In the 2 ⩽ pH ⩽ 4.5 range, $R_{ct,bare}$ is higher than $R_{ct,SAM}$, which is opposite to the relation obtained for pH > 4.5. This can be explained taking into account that for pH < 4.5, electrostatic attraction between the negative species of the redox probe and an increasing fraction of positive charge on the 2-MNA SAM should take place. This, in turn, increases the rate of the charge transfer reaction making that $R_{ct,SAM}$ decreases to values even lower than those for the bare gold substrate. This effect must be assigned undoubtedly to the development of positive charge on the 2-MNA surface species as pH decreases. The positive charge fraction on the monolayer should be generated by the protonation of the pyridinic nitrogen, which takes place overlapped with the protonation of the carboxylate group due to the small difference in pK_a values for both groups. This can also be deduced from the wide pH range that shows the whole change of R_{ct} with pH, which is around four units (from 3.5 to 7.5). Additionally, the progressive protonation of the pyridine nitrogen must be accompanied by desorption of this group from the surface allowing the formation of the zwitterionic for of 2-MNA by intramolecular proton transfer between the nitrogen of the ring and the carboxylic acid group. This would lead, in turn, to a change in the orientation of 2-MNA species at the surface. This is further supported by SERS spectra obtained for SAMS prepared by immersion in 2-MNA solution at pH 13 and afterwards immersed in neutral (pH 7) of acidic (pH 4) solutions (Fig. 5c). Besides the "in-plane" vibration modes enhancement mentioned before, SERS spectra obtained at pH 7 or 4 show a weak enhancement of the bands for the carboxylate stretching ($\nu_s COO^-$ at 1383 cm^{-1}) and bending (δCOO^- at 854 cm^{-1}) vibrations as well as the absence of the carbonyl stretching, $\nu C{=}O$ at 1680 cm^{-1} of the COOH group.

These results indicate that for pH ⩽ 7, at least a fraction of 2-MNA molecules interact perpendicularly to the surface via the thiolate bond and the carboxylate group. Additionally, they also indicate that the carboxylic acid group is found deprotonated when it interacts with the gold surface, even at pH < pK_a. In addition to the electrochemical results, the spectroscopic evidences described above are interpreted as 2-MNA adsorption on gold surfaces at pH ⩽ 7 acquiring two different configurations as summarized in Scheme 2. Similar results have been shown in SERS studies of o-mercaptobenzoic acid [73] and nicotinic acid isomers [74] adsorbed onto Ag.

Nevertheless, it would be emphasized that neither the equilibrium constant value for the formation of the zwitterionic species on the surface nor the effect of pH on this equilibrium are known.

3.3.2. pH effects on the reductive desorption

Reductive desorption of alkanethiol SAMs from a metal surface in aqueous alkaline solutions has been widely used to make a diagnostic of the state of SAMs, and the role of the intermolecular interaction between adsorbed species in determining the peak potential has been discussed [75]. In addition, the difference in the adsorption Gibbs energy of alkanethiolates in the peak shift with the alkyl chain length [76] as well as the existence of nucleation and growth processes at the onset of the reductive desorption [77] have been recognized.

The modeling of the reductive desorption has been described as a one-electron reduction followed by the desorption of the alkanethiolate reduced species from the surface [50]. Assuming that the desorption process is fast enough, a model of a one-step one-electron reductive desorption employing different isotherms in order to incorporate the effect of intermolecular interactions to the rate equations has been employed by Kakiuchi et al. [50] and the conditions for reversible behavior have been discussed. The numerical calculated cyclic voltammograms describe satisfactorily the results for reductive desorption of self-assembled alkanethiols of different chain length in aqueous solutions [50] as well as in ionic liquids [78].

Reductive desorption of SAMs of thiols is also a useful way to evaluate properties such as the pK_a values of the different functional groups in the adsorbed molecules. From a general point of view, during reductive desorption in strong alkaline media of any monolayer of a thiol molecule chemically adsorbed to a gold surface, the electron transfer from the metal surface to the adsorbed molecule is usually described by the reaction:

$$RS - Au + e^- \leftrightarrow RS^- + Au \quad (2)$$

where *R* represents an aromatic group or an aliphatic chain, and the thiolate anions are completely dissolved in the solution after desorption from the surface.

However, as pH of the electrolyte is lowered, protonation of the thiolate group and/or any other ionisable groups in the molecule may take place after the desorption reaction [79,80]

$$RS^- + H^+ \leftrightarrow R - SH \quad (3)$$

Thus, in this case the overall desorption reaction should be formulated as:

$$RS - Au + H^+ + e^- \leftrightarrow R - SH + Au \quad (4)$$

Therefore, according to the pK_a values of the adsorbed and dissolved thiol species, reductive desorption should be pH-dependent. Thus, for reaction (2) the Nernst equation predicts a constant value for the half-wave potential ($E_{1/2}$), while a shifting of −59 mV/pH is expected for reaction (4). Even though a precise analysis of the electrochemical desorption of thiol SAMs cannot be made only by Nernst equation because it is not a simple reversible redox reaction, this approach has been successfully applied to desorption of a number of ω-functionalised thiols adsorbed on gold [79].

In order to gain a deeper insight in the 2-MNA adsorption onto Au(1 1 1) surfaces and the pK_a values of the adsorbed and/or dissolved species, reductive desorption experiments varying the pH of the electrolyte employed for the desorption were performed. Fig. 6 shows the cathodic sweeps obtained in aqueous solutions of different pH for the reductive desorption of 2-MNA SAMs prepared by dipping in an alkaline solutions (pH 13). For desorption at pH 13, a single cathodic peak (peak I) is obtained, as described in Section 3.1 (desorption charge Q_c = 47.0 μC cm^{-2}). In the 13–10 pH range, peak I shows the same characteristics already described, i.e. cathodic charge and peak potential are nearly constant with pH. Below pH 10, peak I shifts progressively towards less negative potentials, showing both a decrease in height and a slight

broadening. At even lower pH values (below around pH 8) the shifting of peak I with pH is more marked and a shoulder (Ib) located at more negative potentials than peak I, is seen. This makes that peak I splits in two broad current contributions (I and Ib), even though the value of Q_c remains constant. At pH 7, peak I is located at −0.46 V (Q_c, I = 24 μC cm^{-2}) and peak Ib appears at −0.56 V (Q_c, Ib = 23 μC cm^{-2}), while at pH 4, peak Ib is predominant and the overall desorption charge decreases slightly. The other remarkable effect observed is the steady increase of the half-peak width as pH decreases. These results can be explained assuming that for adsorbed 2-MNA on Au(1 1 1) only one configuration is present in very alkaline conditions, meanwhile two different structures (I and Ib), with distinct stability, would coexist on the gold surface when neutral or acidic media are employed, as shown in Scheme 2.

Thus, when reductive is performed in neutral or acidic media, peak I corresponds to desorption of the structure where interaction with the gold surface is by sulfur and nitrogen groups, while peak Ib is associated with the other, more stable, configuration. These conclusions are further supported by the results obtained from the titration curve as well as the spectroscopic evidence on 2-MNA interactions with the Au(1 1 1) surface.

In order to lighten the complex dependence of the cathodic desorption profiles on solution pH, the dependence of the peak potential with pH was analyzed. Fig. 7 shows the change of E_p for peaks I and Ib with pH for 2-MNA monolayers prepared by 1 h of immersion in 10 mM 2-MNA + 0.1 M NaOH solutions and desorbed in 0.1 M buffered phosphate solutions of different pH. For peak I the E_p – pH dependence is complex, showing four different zones along the 2–13 pH range studied. In the 10 < pH < 13 range a pH independent value E_p, I = −0.76 V followed by a linear decrease of E_p, I with a slope of around – 60 mV/pH in the 8 < pH < 10 range, are obtained. For 6 < pH < 8, an additional linear decrease of E_p, I with a slope of −120 mV/pH is seen, followed by another region for pH < 6 where the slope is around −38 mV/pH. On the other hand, in the 2 < pH < 7 range, a single dependence of E_p, Ib with a slope of around −55 mV/pH is obtained.

Assuming the one-electron reduction followed by the desorption of the alkanethiolate reduced species from the surface and taking into account the protonation of the thiolate group and/or any other ionisable groups in the molecule that could take place after desorption, the dependence with pH of the peak potential for desorption can be obtained [79]. Thus, for 2-MNA monolayer desorption performed in alkaline media (pH > pK_{a3}), the adsorbed species is not protonated and desorbs from the surface giving the doubly-charged anion according to:

$$Au - S(C_5H_3N)COO^- + e^- \leftrightarrow {}^-S(C_5H_3N)COO^- + Au \quad (5)$$

As a consequence, in this pH range desorption of 2-MNA is pH-independent and a constant value of E_p is expected. However, there are also other groups, i.e. thiol, carboxylate and pyridinic groups, that depending on solution pH can be protonated/deprotonated after desorption of the monolayer. For pH < pK_{a3} protonation of the thiolate group in solution should take place after desorption, according to the overall reaction:

$$Au - S(C_5H_3N)COO^- + H^+ + e^- \leftrightarrow HS - (C_5H_3N)COO^- + Au \quad (6)$$

and a linear E_p vs. pH variation with a slope of −60 mV/pH is predicted [62]. This is the behavior found for peak I in the 10–8 pH range. The bending at pH ≈ 10 can be associated with the pK_a value for the thiol group, in fair agreement with the value pK_{a3} = 11 reported in Ref. [67].

Below pH ≈ 8, another break in the E_p, I vs. pH plot, which extends up to pH ≈ 6, is obtained. In this pH range, carboxylate group is not fully protonated since pK_{a2}(SAM) ≈ 6 as estimated from the titration curve in Section 3.3.1. However, if the value of pK_{a2} = 7.4 from Ref. [67] is considered, after desorption both the thiol as well as the carboxylate groups must be protonated in solution, according to:

$$Au - S(C_5H_3N)COO^- + 2H^+ + e^- \leftrightarrow HS - (C_5H_3N)COOH + Au \quad (7)$$

For this reaction scheme, a linear E_p vs. pH dependence with a slope of −120 mV/pH is expected, as experimentally found (Fig. 7). These results also allow to assign the value pK_{a2}(SAM) ≈ 6 for the carboxylate group for the self-assembled layer of 2-MNA. Finally, for pH < 6 the carboxylate group for the adsorbed 2-MNA layer is protonated, and desorption can be represented by:

$$Au - S(C_5H_3N)COOH + H^+ + e^- \leftrightarrow HS - (C_5H_3N)COOH + Au \quad (8)$$

and a linear dependence with a slope of – 60 mV/pH is predicted. However, the value obtained is around −38 mV/pH, which has been explained by an additional stabilization of the SAM due to lateral interactions, probably as a consequence in the present case, of hydrogen bonding between adjacent molecules [79].

On the other hand, as pK_{a2}(SAM) ≈ 6 and taking into account that protonation/deprotonation equilibria take place in the range of pK ± 1, the initiation of the protonation of the carboxylate group at adsorbed species takes place around pH 7. Therefore, a this pH value the formation of zwitterionic adsorbed species is possible as discussed above. This leads to protonation of the pyridinic nitrogen with loss of the nitrogen interaction with the surface as well as to the carboxylate group interaction with the gold substrate (Scheme 2). In acidic solutions, the two other structures (I and Ib) probably exist forming different domains on the surface. The desorption process of the zwitterionic adsorbed species (structure Ib) takes place at potentials more negative than for peak I, which would mean that an important interaction of carboxylate group with the gold surface takes place.

For this case, desorption can be represented by the reaction:

$$Au - S(C_5H_3NH^+)COO^- + H^+ + e^- \leftrightarrow HS - (C_5H_3NH^+)COO^- + Au \quad (9)$$

A linear E_p vs. pH variation with a slope of −60 mV/pH is expected, which is very similar to the value of −55 mV/pH found in the 2–7 pH range for peak Ib (Fig. 8).

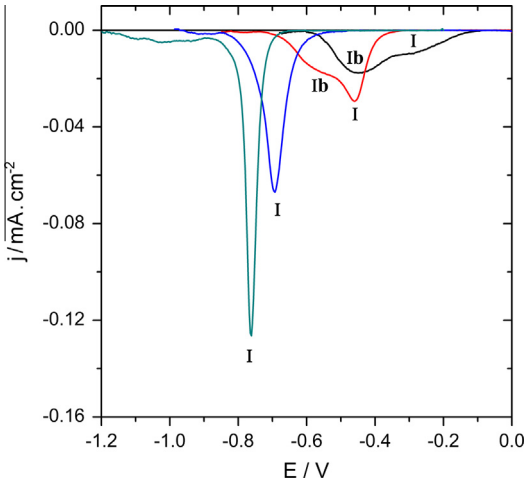

Fig. 7. Reductive desorption at 0.1 V s^{-1} in 0.1 M NaOH (——) or in 0.1 M buffered phosphate solutions of pH 9 (——); 7 (——) and 4 (——) for Au(1 1 1) surfaces modified after 1 h of dipping in a 10 mM 2-MNA solution (pH 13). The reader is referred to the web version of this article for interpretation of this figure.

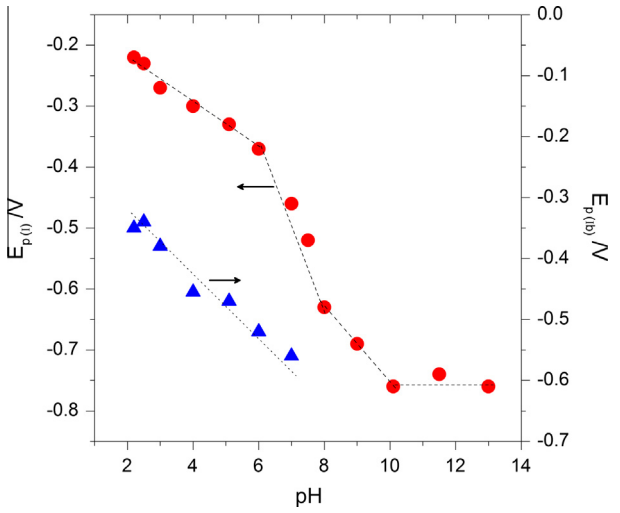

Fig. 8. pH dependence of E_p for peak I (●) and Ib (▲) for the reductive desorption at 0.1 V s^{-1} of 2-MNA monolayers prepared on Au(1 1 1) for 1 h of dipping in 0.1 M NaOH (pH 13).

4. Conclusions

Potentiodynamic *j*/*E* response of self-assembled 2-mercaptonicotinic acid monolayers on Au(1 1 1) in alkaline solutions shows characteristic desorption/re-adsorption waves. 2-MNA desorbs reductively from the surface at −0.76 V (vs. ECS). From desorption experiments the value of the surface concentration can be estimated, which result similar to that reported for related aromatic molecules.

The change of the kinetics of the electron transfer reaction for the Fe^{2+}/Fe^{3+} redox probe in the presence of the SAM provides structural information of the monolayers. Both, cyclic voltammetry and electrochemical impedance spectroscopy measurements, show a rather imperfect blocking behavior of the 2-MNA SAM. This behavior corresponds to that obtained for microelectrode arrays, which is attributed to the access of ions through pinholes, defects and/or pores present in the SAM. From EIS experiments an estimation of coverage is made, obtaining an increase of coverage with dipping time, indicating a higher stabilization and packing of the monolayer as dipping time increases.

In aqueous solution, 2-mercaptonicotinic acid behaves as a weak acid presenting a complex acid–base behavior as well as equilibrium reactions between tautomeric species, including the formation of zwitterionic forms. In strong alkaline aqueous solutions, 2-MNA stable species corresponds mainly to the doubly-charged negative species and a strong thiolate-gold chemical bond as well as a moderate interaction involving the non-bonding electrons of the non-protonated pyridinic nitrogen with the gold surface are expected. Additionally, no interaction of the surface with the carboxylate group is detected by SERS.

The characteristics of ionisable groups exposed to the solution in the 2-MNA monolayers prepared by dipping in alkaline solutions were obtained by impedance measurements at different pH using the $[Fe(CN)_6]^{3-}/[Fe(CN)_6]^{4-}$ redox probe. A value $pK_{a(SAM)} \approx 6.0$ can be estimated for the carboxylate group in the surface 2-MNA monolayer, indicating that for pH > pK_a, the carboxylic acid group is deprotonated and the monolayer acquires a negative surface charge, meanwhile it remains neutral or positively charged at lower pH values due to the beginning of pyridinic nitrogen protonation. From the comparison of R_{ct} variation with pH obtained for the bare and modified gold surfaces, it is concluded that for pH < 4.5, an increasing fraction of positive charge on the 2-MNA SAM takes place due to protonation of the pyridinic nitrogen, which takes place overlapped with the protonation of the carboxylate group. The protonation of the pyridinic nitrogen must be accompanied by desorption of this group from the surface, allowing the formation of the zwitterionic species of 2-MNA by intramolecular proton transfer between the nitrogen of the ring and the carboxylic acid group. This leads to a change in the orientation of 2-MNA species allowing the interaction between the carboxylate group and the gold surface, which is further corroborated from SERS measurements.

Reductive desorption of SAMs of thiols at different pH values was also employed to evaluate properties as pK_a values of the different functional groups in the adsorbed molecules. As pH of the electrolyte is lowered, protonation of the thiolate group and/or any other ionisable groups in the molecule may take place after the desorption process, resulting in a pH-dependent value of peak potential for reductive desorption. In alkaline aqueous medium, 2-MNA adsorbs through a thiolate chemical bond on the gold surface and an additional interaction of the pyridinic nitrogen stabilizes the monolayer. Thus, when reductive desorption is made in alkaline medium, only one cathodic peak is obtained. Also, this configuration exposes the carboxylate group to the solution, which can be protonated when pH is lowered below 8. Furthermore, the splitting in two cathodic current contributions for pH values lower than ca. 7, allows to state that two different molecular configurations for 2-MNA coexist on the gold surface in neutral or acidic media. This is assigned to the occurrence of an equilibrium between the molecular structure bonded through sulfur and nitrogen and the surface-bonded zwitterionic species by intramolecular proton transfer from the carboxylic acid group to the ring nitrogen, leading to the protonation of the pyridinic nitrogen and allowing the interaction of the carboxylate group with the gold surface.

Acknowledgements

Financial support from the Consejo Nacional de Investigaciones Científicas y Técnicas of Argentina (CONICET), the Agencia Nacional de Promoción Científica y Tecnológica (ANPCYT), the Secretaría de Ciencia y Tecnología (SECYT-UNC) and FONCYT PME 2006-1544, is gratefully acknowledged. DEP thanks CONICET for the fellowships granted.

References

[1] Q. Jin, J.A. Rodríguez, C.Z. Li, Y. Darici, N.J. Tao, Self-assembly of aromatic thiols on Au(1 1 1), Surf. Sci. 425 (1999) 101–111.
[2] E. Sabatani, J. Cohen-Boulakia, M. Bruening, I. Rubinstein, Thioaromatic monolayers on gold: a new family of self-assembling monolayers, Langmuir 9 (1993) 2974–2981.
[3] C. Retna Raj, T. Ohsaka, Voltammetric detection of uric acid in the presence of ascorbic acid at a gold electrode modified with a self-assembled monolayer of heteroaromatic thiol, J. Electroanal. Chem. 540 (2003) 69–77.
[4] C. Amatore, J.M. Savéant, D. Tessier, Charge transfer at partially blocked surfaces. A model for the case of microscopic active and inactive sites, J. Electroanal. Chem. 147 (1983) 39–51.
[5] H.O. Finklea, D.A. Snider, J. Fedik, E. Sabatani, Y. Gafni, I. Rubinstein, Characterization of octadecanethiol-coated gold electrodes as microarray electrodes by cyclic voltammetry and ac impedance spectroscopy, Langmuir 9 (1993) 3660–3667.
[6] E. Sabatani, I. Rubinstein, Organized self-assembling monolayers on electrodes. 2. Monolayer-based ultramicroelectrodes for the study of very rapid electrode kinetics, J. Phys. Chem. 91 (1987) 6663–6669.
[7] X. Lu, H. Yuan, G. Zuo, J. Yang, Study of the size and separation of pinholes in the self-assembled thiol-porphyrin monolayers on gold eelctrodes, Thin Solid Films 516 (2008) 6476–6482.
[8] A.A.P. Ferreira, C.S. Fugivara, S. Barrozo, P.H. Suegama, H. Yamanaka, A.V. Benedetti, Electrochemical and spectroscopic characterization of screen-printed gold-based electrodes modified with self-assembled monolayers and Tc85 protein, J. Electroanal. Chem. 634 (2009) 111–122.
[9] V. Ganesh, R.R. Pandey, B.D. Malhotra, V. Lakshminarayanan, Electrochemical characterization of self-assembled monolayers (SAMs) of thiophenol and

aminothiophenols on polycrystalline Au: effects of potential cycling and mixed SAM formation, J. Electroanal. Chem. 619 (2008) 87–97.
[10] P. Diao, M. Guo, R. Tong, Characterization of defects in the formation process of self-assembled thiol monolayers by electrochemical impedance spectroscopy, J. Electroanal. Chem. 495 (2001) 98–105.
[11] S. Campuzano, M. Pedrero, C. Montemayor, E. Fatás, J.M. Pingarrón, Characterization of alkanethiol self-assembled monolayers-modified gold electrodes by electrochemical impedance spectroscopy, J. Electroanal. Chem. 586 (2006) 112–121.
[12] V. Ganesh, V. Lakshminarayanan, Scanning tunneling microscopy, Fourier transform infrared spectroscopy, and electrochemical characterization of 2-naphtalenethiol self-assembled monolayers on the Au surface: a stucy of bridge mediated electron transfer in $Ru(NH_3)_6^{2+}/Ru(NH_3)_6^{3+}$ redox reaction, J. Phys. Chem. B 109 (2005) 16372–16381.
[13] C. Mokrani, J. Fatisson, L. Guérente, P. Labbé, Structural characterization of (3-mercaptopropyl)sulfonate monolayer on gold electrodes, Langmuir 21 (2005) 4400–4409.
[14] R.P. Janek, W. Ronald Fawcett, A. Ulman, Impedance spectroscopy of self-assembled monolayers on Au(111): sodium ferrocyanide charge transfer at modified electrodes, Langmuir 14 (1998) 3011–3018.
[15] D. García-Raya, R. Madueño, J.M. Sevilla, M. Blázquez, T. Pineda, Electrochemical characterization of a 1,8-octanedithiol self-assembled monolayer (ODT-SAM) on a Au(111) single crystal electrode, Electrochim. Acta 53 (2008) 8026–8033.
[16] V. Ganesh, S. Kumar Pal, S. Kumar, V. Lakshminarayanan, Self-assembled monolayers (SAMs) of alkoxycyanobiphenyl thiols on gold – a study of electron transfer reaction using cyclic voltammetry and electrochemical impedance spectroscopy, J. Colloid Interf. Sci. 296 (2006) 19–5203.
[17] C. Retna Raj, S. Behera, Electrochemical studies of 6-mercaptonicotinic acid monolayer on Au electrode, J. Electroanal. Chem. 581 (2005) 61–69.
[18] H.O. Finklea, Electrochemistry of organized monolayers of thiols and related molecules on electrodes, in: A.J. Bard, I. Rubinstein (eds.) Electroanal. Chem.: A series of Advances, vol. 19, Marcel Dekker Inc., New York, 1996, pp. 109–335.
[19] H.S. White, J.D. Peterson, Q. Cui, K.J. Stevenson, Voltammetric measurement of interfacial acid/base reactions, J. Phys. Chem. B 102 (1998) 2930–2934.
[20] T. Kakiuchi, M. Lida, S.I. Imabayashi, K. Niki, Double-layer-capacitance titration of self-assembled monolayers of ω-functionalized alkanethiols on Au(111) surface, Langmuir 16 (2000) 5397–5401.
[21] S.E. Creager, J. Clarke, Contact-angle titrations of mixed ω-mercaptoalkanoic acid/alkanethiol monolayers on gold, reactive vs nonreactive spreading and chain length effects on surface pK_a values, Langmuir 10 (1994) 3675–3683.
[22] J. Wang, L.M. Frostman, M.D. Ward, Self-assembled thiol monolayers with carboxylic acid functionality: measuring pH-dependent phase transitions with the quartz crystal microbalance, J. Phys. Chem. 96 (1992) 5224–5228.
[23] O. Gershevitz, C.N. Sukenik, In situ FTIR-ATR analysis and titration of carboxylic acid-terminated SAMs, J. Am. Chem. Soc. 126 (2004) 482–483.
[24] J. Pillay, B.O. Agboola, K.I. Ozoemena, Electrochemistry of 2-dimethyl-aminoethanethiol SAM on gold electrode: Interaction with SWCNT-poly(*m*-aminobenzene sulphonic acid), electric field-induced protonation–deprotonation, and surface pK_a, Electrochem. Commun. 11 (2009) 1292–1296.
[25] S.C. Burris, Y. Zhou, W.A. Maupin, A.J. Ebelhar, M.W. Daugherty, The effect of surface preparation on apparent surface pK_a's of ω-mercaptocarboxylic acid self-assembled monolayers on polycrystalline gold, J. Phys. Chem. C 112 (2008) 6811–6815.
[26] D.D. Justino, A.L. Almeida Lage, D.E. Pires Souto, J. Vieira da Silva, W. Torres, P. dos Santos, R. Silva Luz, F.S. Damos, Study of the effects of surface pK_a and electron transfer kinetics of electroactive 4-nitrothiophenol/4-mercaptobenzoic acid binary SAM on the simultaneous determination of epinephrine and uric acid, J. Electroanal. Chem. 703 (2013) 158–165.
[27] R.A. Clark, C.J. Trout, L.E. Ritchey, A.N. Marciniak, M. Weinzierl, C.N. Schirra, D.C. Kurtz, Electrochemical titration of carboxylic acid terminated SAMs on evaporated gold: understanding the ferricyanide electrochemistry at the electrode surface, J. Electroanal. Chem. 689 (2013) 284–290.
[28] B.W. Park, D.Y. Yoon, D.S. Kim, Formation and modification of a binary self-assembled monolayer on a nano-structured gold electrode and its structural characterization by electrochemical impedance spectroscopy, J. Electroanal. Chem. 661 (2011) 329–335.
[29] F.P. Cometto, C.A. Calderón, E.M. Euti, D.K. Jacquelín, M.A. Pérez, E.M. Patrito, V.A. Macagno, Electrochemical study of adlayers of α, ω-alkanedithiols on Au(111): influence of the forming solution, chain length and treatment with mild reducing agents, J. Electroanal. Chem. 661 (2011) 90–99.
[30] J. Cancino, S.A.S. Machado, Microelectrode array in mixed alkanethiol self-assembled monolayers: electrochemical studies, Electrochim. Acta 72 (2012) 108–113.
[31] F.P. Cometto, E.M. Patrito, P. Paredes Olivera, G. Zampieri, H. Ascolani, Electrochemical, high-resolution photoemission spectroscopy and vdW-DFT study of the thermal stability of benzenethiol and benzeneselenol monolayers on Au(111), Langmuir 28 (2012) 13624–13635.
[32] E. Pensa, A.A. Rubert, G. Benítez, P. Carro, A. González Orive, A. Hernández Creus, R.C. Salvarezza, C. Vericat, Are 4-mercaptobenzoic acid self assembled monolayers on Au(111) a suitable system to test adatom models?, J Phys. Chem. C 116 (2012) 25765–25771.
[33] T.deF. Paulo, H.D. Abruña, I.C.N. Diógenes, Thermodynamic, kinetic, surface pK_a, and structural aspects of self-assembled monolayers of thio compounds on gold, Langmuir 28 (2012) 17825–17831.
[34] J.M. Campina, A. Martins, F. Silva, Probing the organization of charged self-assembled monolayers by using the effects of pH, time, electrolyte anion, and temperature, on the charge transfer of electroactive probes, J. Phys. Chem. C 113 (2009) 2405–2416.
[35] S.C. Burris, Y. Zhou, W.A. Maupin, A.J. Ebelhar, M.W. Daugherty, The effect of surface preparation on apparent surface pK_a's of ω-mercaptocarboxilic acid self-assembled monolayers on polycrystalline gold, J. Phys. Chem. C 112 (2008) 6811–6815.
[36] R. Madueño, D. García-Raya, A.J. Viudez, J.M. Sevilla, T. Pineda, M. Blázquez, Influence of the solution pH in the 6-mercaptopurine self-assembled monolayer on a Au(111) single-crystal electrode, Langmuir 23 (2007) 11027–11033.
[37] F. Björefors, R.M. Petoral, K. Uvdal, Electrochemical impedance spectroscopy for investigations on ion permeation in ω-functionalized self-assembled monolayers, Anal. Chem. 79 (2007) 8391–8398.
[38] H.Z. Yu, N. Xia, Z.F. Liu, SERS titration of 4-mercaptopyridine self-assembled monolayers at aqueous buffer/gold interfaces, Anal. Chem. 71 (1999) 1354–1358.
[39] D.A. Smith, M.L. Wallwork, J. Zhang, J. Kirkham, C. Robinson, A. Marsh, M. Wong, The effect of electrolyte concentration on the chemical force titration behavior of ω-functionalized SAMs: evidence for the formation of strong ionic hydrogen bonds, J. Phys. Chem. B 104 (2000) 8862–8870.
[40] M.A. Bryant, R.M. Crooks, Determination of surface pK_a values of surface-confined molecules derivatized with pH-sensitive pendant groups, Langmuir 9 (1993) 385–393.
[41] N.K. Chaki, M. Aslam, J. Sharma, K. Vijayamohanan, Applications of self-assembled monolayers in materials chemistry, Proc. Indian Acad. Sci. 113 (2001) 659–670.
[42] H.I.S. Nogueira, Surface-enhanced Raman scattering (SERS) of 3-aminosalicylic and 2-mercaptonicotinic acids in silver colloids, Spectrochim. Acta Part A 54 (1998) 1461–1470.
[43] K.H. Yu, J.M. Rhee, Y. Lee, K. Lee, S. Yu, Surface-enhanced Raman scattering study of 4-biphenylcarboxylic acid, Langmuir 17 (2001) 52–55.
[44] N.G. Tognalli, A. Fainstein, C. Vericat, M.E. Vela, R.C. Salvarezza, Exploring three-dimensional nanosystems with Raman spectroscopy: methylene blue adsorbed on thiol and sulfur monolayers on gold, J. Phys. Chem. B 110 (2006) 354–360.
[45] J. Gao, Y. Hu, S. Li, Y. Zhang, X. Chen, Adsorption of benzoic acid, phthalic acid on gold substrates studied by surface-enhanced Raman scattering spectroscopy and density functional theory calculations, Spectrochim. Acta Part A 104 (2013) 41–47.
[46] E. Tan, P Yin, X. Lang, H. Zhang, L. Guo, A novel surface-enhanced Raman scattering nanosensor for detecting multiple heavy metal ions based on 2-mercaptoisonicotinic acid functionalized gold nanoparticles, Spectrochim. Acta Part A 97 (2012) 1007–1012.
[47] N. Hassan, R. Holze, Surface enhanced Raman spectroscopy of self-assembled monolayers of 2-mercaptopyridine on a gold electrode, Russ. J. Electrochem. 48 (2012) 401–411.
[48] E.B. Wilson, The normal modes and frequencies of vibration of the regular plane hexagon model of the benzene molecule, Phys. Rev. 45 (1934) 706–714.
[49] R.C. Lord, A.L. Marston, F.A. Miller, Infra-red and Raman spectra of the diazines, Spectrochim. Acta 9 (1957) 113–125.
[50] T. Kakiuchi, H. Usui, D. Hobara, M. Yamamoto, Voltammetric properties of the reductive desorption of alkanethiol self-assembled monolayers from a metal surface, Langmuir 18 (2002) 5231–5238.
[51] L. Wan, M. Terashima, H. Noda, M. Osawa, Molecular orientation and ordered structure of benzenethiol adsorbed on gold(111), J. Phys. Chem. B 104 (2000) 3563–3569.
[52] I. Taniguchi, H. Ishimoto, K. Miyagawa, M. Iwai, H. Nagai, H. Hanazono, K. Taira, A. Kudo, A. Nishikawa, K. Nishiyama, Z. Dursun, G.P.-J. Hareau, M. Tazaki, Surface functions of 2-mercaptopyridine, 2-mercaptopyrazine and 2-mercaptoquinoxaline modified Au(111) electrodes for direct rapid electron transfer of cytochrome c, Electrochem. Commun. 5 (2003) 857–861.
[53] T. Sawaguchi, F. Mizutani, S. Yoshimoto, I. Taniguchi, Voltammetric and in situ STM studies on self-assembled monolayers of 4-mercaptopyridine, 2-mercaptopyridine and thiophenol on Au(111) electrodes, Electrochim. Acta 45 (2000) 2861–2867.
[54] S. Yoshimoto, T. Sawaguchi, F. Mizutani, I. Taniguchi, STM and voltammetric studies on the structure of a 4-pyridinethiolate monolayer chemisorbed on Au(100)–(1 × 1) surface, Electrochem. Commun. 2 (2000) 39–43.
[55] C. Zhong, M. Porter, Evidence for carbon-sulfur bond cleavage in spontaneously adsorbed organosulfide-based monolayers at gold, J. Am. Chem. Soc. 116 (1994) 11616–11622.
[56] Y. Sato, F. Mizutani, Formation and characterization of aromatic selenol and thiol monolayers on gold: in situ IR studies and electrochemical measurements, Phys. Chem. Chem. Phys. 6 (2004) 1328–1331.
[57] L.J. Wan, M. Terashima, H. Noda, M. Osawa, Molecular orientation and ordered structure of benzenethiol adsorbed on gold (111), J. Phys. Chem. B 104 (2000) 3563–3569.
[58] D.G. Matei, H. Muzik, A. Golzhauser, A. Turchanin, Structural investigation of 1,1′-biphenyl-4-thiol self-assembled monolayers on Au(111) by scanning tunneling microscopy and low-energy electron diffraction, Langmuir 28 (2012) 13905–13911.
[59] B. Lamp, D. Hobara, M. Porter, K. Niki, T. Cotton, Correlation of the structural decomposition andpPerformance of pyridinethiolate surface modifiers at gold electrodes for the facilitation of Cytochrome *c* heterogeneous electron-transfer reactions, Langmuir 13 (1997) 736–739.

[60] D. Weisshaar, M. Walczak, M. Porter, Electrochemically induced transformations of monolayers formed by self-assembly of mercaptoethanol at gold, Langmuir 9 (1993) 323–331.
[61] F.P. Cometto, V.A. Macagno, P. Paredes-Olivera, E.M. Patrito, H. Ascolani, G. Zampieri, Decomposition of methyltiolate monolayers on Au(1 1 1) prepared from dimethylsulfide in solution phase, J. Phys. Chem. C 114 (2010) 10183–10194.
[62] A.J. Bard, L.R. Faulkner, Electrochemical Methods. Fundamentals and Applications, second ed., John Wiley Inc., N. York, 2001.
[63] R.S. Nicholson, I. Shain, Theory of stationary electrode polarography. Single Scan and cyclic methods applied to reversible, irreversible, and kinetic Systems, Anal. Chem. 36 (1964) 706–723.
[64] I.A. Raistrick, D.R. Franceschetti, J. Ross Macdonald, in: E. Barsoukov, J. Ross Macdonald (Eds.), Impedance Spectroscopy. Theory, Experiment and Applications, second ed., J. Wiley & Sons Inc., N. Jersey, 2005, pp. 27–128.
[65] Gerald D. Fasman, Handbook of Biochemistry and Molecular Biology, 3rd Edition., CRC Press, 1977.
[66] M.G. Saleh, K.A. Idriss, M.S. Abu-Bakr, E.Y. Hashem, Acid dissociation and solution equilibria of some pyridinecarboxylic acids, Analyst 117 (1992) 1003–1007.
[67] J.F. Read, C.R. Graves, E. Jackson, The kinetics and mechanism of the oxidation of the thiols 3-marcapto-1-propane sulfonic and 2-mercaptonicotinic acid by potassium ferrate, Inorg. Chim. Acta 348 (2003) 41–49.
[68] Y.S. Pang, H.J. Hwang, M.S. Kim, Adsorption of 2-mercaptopyridine and 2-mercaptopyrimidine on a silver colloidal surface investigated by Raman Spectroscopy, J. Mol. Struct. 441 (1998) 63–76.
[69] L. Wan, H. Noda, Y. Hara, M. Osawa, Effect of solution pH on the structure of a 4-mercaptopyridine monolayer self-assembled on Au(1 1 1), J. Electroanal. Chem. 489 (2000) 68–75.
[70] K. Kim, J. Kwak, Faradaic impedance titration of pure 3-mercaptopropionic acid and ethanethiol mixed monolayers on gold, J. Electroanal. Chem. 512 (2001) 83–91.
[71] R. Madueño, D. García-Raya, J. Viudez, J. Sevilla, T. Pineda, M. Blazquez, Influence of the solution pH in the 6-mercaptopurine self-assembled monolayer (6MP-SAM) on a Au(1 1 1) single-crystal electrode, Langmuir 23 (2007) 11027–11033.
[72] H. Bruhn, S. Nigam, J.F. Holzwarth, Catalytic influence of the environment on outer-sphere electron-transfer reactions in aqueous solutions, Faraday Discuss. Chem. Soc. 74 (1982) 129–140.
[73] S.B. Lee, K. Kim, M.S. Kim, Surface-enhanced Raman scattering of o-mercaptobenzoic acid in silver sol, J. Raman Spectrosc. 22 (1991) 811–817.
[74] R. Wen, Y. Fang, Adsorption of pyridine carboxylic acids on silver surface investigated by potential-dependent SERS, Vibrational Spectrosc. 39 (2005) 106–113.
[75] S. Imabayashi, M. Iida, D. Hobara, Z.Q. Feng, K. Niki, T. Kakiuchi, Reductive desorption of carboxylic-acid-terminated alkanethiol monolayers from Au(1 1 1) surfaces, J. Electroanal. Chem. 428 (1997) 33–38.
[76] D.W. Hatchet, K.J. Stevenson, W.B. Lacy, J.M. Harris, H.S. White, Electrochemical oxidative adsorption of ethanethiolate on Ag(1 1 1), J. Am. Chem. Soc. 119 (1997) 6596–6606.
[77] N. Mohtat, M. Byloos, M. Soucy, S. Morin, M. Morin, Electrochemical evidence of the adsorption of alkanethiols on two sites on Ag(1 1 1), J. Electroanal. Chem. 484 (2000) 120–130.
[78] D. Oyamatsu, T. Fujita, S. Arimoto, H. Munakata, H. Matsumoto, S. Kuwabata, Electrochemical desorption of a self-assembled monolayer of alkanethiol in ionic liquids, J. Electroanal. Chem 615 (2008) 110–116.
[79] H. Munakata, D. Oyamatsu, S. Kuwabata, Effects of ω-functional groups on pH-dependent reductive desorption of alkanethiol self-assembled monolayers, Langmuir 20 (2004) 10123–10128.
[80] H. Munakata, S. Kuwabata, Detection of difference in acidity between arrayed carboxy groups and the groups dissolved in solution by reductive desorption of a self-assembled monolayer of carboxy-terminated thiols, Chem. Commun. (2001) 1338–1339.